Sādhanā (2020) 45:102
https://doi.org/10.1007/s12046-020-01347-9
© Indian Academy of Sciences

Microstructure evolution of interface between magnesium ammonium phosphate cement and Portland cement under sulphate corrosion environment

JUN LI[1,2,3,4,*], YONG-SHENG JI[2] and ZHISHAN XU[2]

[1]School of Civil Engineering and Architecture, Kaifeng University, Kaifeng 475004, Henan, China
[2]State Key Laboratory for Geomechanics and Deep Underground Engineering, China University of Mining and Technology, Xuzhou 221008, Jiangsu, China
[3]Sponge City Engineering Materials Technology Research Center of Kaifeng, Kaifeng 475004, Henan, China
[4]Collaborative Innovation Center for New Energy-Saving Building Materials of Kaifeng University, Kaifeng 475004, Henan, China
e-mail: l1979394@163.com

MS received 31 July 2019; revised 5 March 2020; accepted 6 March 2020

Abstract. This paper reports the test results on the bonding strength between magnesium ammonium phosphate cement and Portland cement. The bonded specimens were prepared by immersion in Na_2SO_4 solution. Following immersion, the surfaces and positions of fractures on the specimens were examined. SEM and an optical microscope were used to analyse changes of the interfacial microzone following different immersion periods. Microstructure changes of the magnesium ammonium phosphate cement-based interfacial microzone within the bonded mortar specimens were studied and compared with those immersed in normal conditions. The bonded mortar specimens were found to have weaker bonding strength than that of the mortar specimens in normal conditions. Under normal conditions, slight crystal morphology changes of the interfacial microzone were observed and the crystal structure appeared compact, while more noticeable changes occurred within mortar specimens immersed in Na_2SO_4 solution, with the crystal structures within them being more loose. The bonding behaviour of the magnesium ammonium phosphate cement includes mechanical bonding, mutual diffusion, and chemical bonding. Structural diagrams of the interfacial transition zone (ITZ) in different environments are also presented. Further investigations are needed to determine the performance of the bonding interface microzone of Portland cements and magnesium ammonium phosphate cements within repair materials in order to enhance the performance of cement-based composite materials for concrete repair.

Keywords. Repair; interfacial transition zone; bond behaviour; model; evolution.

1. Introduction

There are a lot of salinized soil in the west of China. Salt Lake area in China accounts for more than half of the country's territory. The salt content of salt lake brine is 10–15 times of that of seawater. The average content of SO_4^{2-} in Qinghai Salt Lake is 33200 mg/L and that in Inner Mongolia Salt Lake is 36400 mg/L. In the vast saline soil area, a lot of corrosion damage is produced to the concrete structure. Concrete structures may fail under saline soil environment, making it necessary to repair and maintain these structures. Repair materials must thus possess anti-freezing, anti-permeability and carbonisation capabilities, as well as fine load-bearing capacity.

Currently, commonly used repairing materials include: (1) Mortar and concrete made of ordinary Portland cement and aggregate. The advantage of this kind of repairing material is that the thermal expansion coefficient and elastic modulus are the same as the matrix, but low bond strength and slow-developing early strength are their disadvantages. (2) Organic macromolecule materials, such as epoxy resin. This repair material is advantageous due to strong bonding force, fast setting, and high temperature resistance but disadvantageous because of poor volume compatibility with old concrete, high cost and quick ageing. (3) Special cement, such as sulphoaluminate, alkali-activated and phosphate cements. This inorganic repairing material is characterized by short setting time, high early strength, and similar thermal expansion coefficient and elastic modulus to old concrete.

It is essential to select appropriate materials that are durable and improve mechanical properties. Adding

*For correspondence
Published online: 06 May 2020

magnesium ammonium phosphate cement (MAPC) leads to increased abrasive resistance, high bonding strength, high strength and rapid condensation. It is also a similar colour to that of the existing concrete [1–8]. MAPC binder has been extensively used to repair concrete runways, bridge surfaces, roads, pavements and grounds in industrial plants. Studies [9–21] show that sodium hydroxide and hydrogen chloride solutions corrode MPC-based materials heavily, while sodium chloride sand sodium sulphate solutions corrode MPC-based materials lightly. The pH of salt solutions is equal to that of the hydration products of the MPC system. Therefore, the stability of the hydration products will not be affected. Under the same conditions, the strength of MPC-based materials soaked in magnesium sulphate solution is higher than that of those soaked in sodium sulphate solution. Magnesium sulphate solution infiltrates MPC-based materials, providing Mg^{2+} for the reaction that generates new hydration products and increases the hydration degree of MPC-based materials. However, the performance of the interfacial microzone in repaired concrete when exposed to a high corrosive environment has been seldom studied. This knowledge gap inhibits the application and popularity of MAPC. At the same time, the interfacial microzone has a great influence on the performance of magnesium ammonium phosphate cement when used as repair material and coatings. Therefore, there is a need to investigate the performance of the bonding interface microzone of Portland cements and magnesium phosphate within repair materials in order to enhance the performance of cement-based composite materials for concrete repair.

In this paper, the structure and property evolution of the interface transition zone of MAPC repair mortar specimens were analyzed in a sulphate environment. The structure and property of interface transition zones in a natural environment are compared in order to study the performance of the bonding interface transition zone between MAPC and Portland cement.

2. Experiments

2.1 *Raw materials and mixture ratio*

(1) Cement

P.I: 42.5 Portland cement was used, which was supplied by the Xuzhou Zhonglian Cement Corporation in China and conformed to the Chinese National Standard GB175 (equivalent to European CEM I 42.5). The cement density was 3100 kg/m^3, with a mean particle size of 26.6 um, and a specific surface area of 348 m^2/kg. Table 1 shows the chemical composition of Portland cement.

(2) MAPC

The MAPC was prepared by mixing magnesia oxide powder, $NH_4H_2PO_4$, and a compound retarder to specific proportions in a laboratory, as detailed in section 2.2. The dead burned magnesia (MgO) powder, calcined at >1700°C, was obtained from the Huashan Plant, Shenyang. The specific surface and the powder density were respectively 280 m^2/kg and 3670 kg/m^3. The average particle size was 20 um. The chemical composition of the commercial dead burned MgO is detailed in table 1.

Soluble phosphate, with a purity of greater than 98%, was used as industrial-grade $NH_4H_2PO_4$. The maximum particle size of $NH_4H_2PO_4$ was 700 μm. The compound retarder was prepared in a laboratory and is abbreviated as "B" [22].

The raw materials were mixed with a water-to-cement mass ratio (W/C) of 0.5 to prepare the mortar specimens. In this study, the MAPC paste was prepared by mixing raw materials with a magnesia-to-phosphate molar ratio (M/P) of 4 and a B-to-magnesia molar ratio (B/M) of 0.05. The water-to-cement mass ratio (W/C) of the cement containing magnesia and $NH_4H_2PO_4$ was 0.12. The grouping and mixture ratios are shown in table 2. The workability and strength of magnesium phosphate cement were the best [22].

The powdered materials, MgO, $NH_4H_2PO_4$ and B, were dry-mixed in a mixer pan for 3 min, and then B was added and mixed in for another 1 min.

(3) Other materials

River sand with a fineness modulus of 2.78 and a saturated surface dry specific gravity of 2760 kg/m^{-3} was used as fine aggregate. Potable water was used as mixing water.

Industrial grade Na_2SO_4 was used, with a maximum particle size of 700 μm and purity greater than 98%.

Table 2. Mix of MAPC pastes.

Code name	m_M/m_P	m_B/m_{Mg}	m_W/m_C
M1	4	5%	0.12

Table 1. Chemical composition of Portland cement and magnesium oxide powder/(wt%)

Raw materials	SiO_2	Al_2O_3	Fe_2O_3	CaO	MgO	Na_2O	K_2O	SO_3	Loss
Cement	24.55	7.77	3.62	54.59	2.68	0.31	1.50	2.24	1.2
Magnesium oxide powder	3.68	0	0	3.14	91.85	0	0	0	1.2

2.2 *Specimen preparation*

The proportions in the Portland cement-based mortar specimens were as follows: m(cement):m(sand):m(water) = 1.0:3.0:0.5. The dimensions of these cement mortar specimens were 40 mm × 40 mm × 160 mm. In accordance with the ISO's *Cement Mortar Strength Test Method* (GB/T 1767l-1999) guidelines, the cement mortar specimens were moulded and maintained under natural curing conditions for 28 d.

Surface laitance was removed and the surface was ground with a steel wire brush along an orthogonal direction. Afterwards, half of the Portland cement specimens were placed into a 40 mm × 40 mm × 160 mm mould, and MAPC mortar was cast into the mould with half of the Portland cement specimen. After 1 h, the specimens were removed from the mould and placed into a standard curing room (20°C, 95% relative humidity) to cure under natural curing conditions for 28 d.

2.3 *Test methods and material characteristics*

A total of 15 repaired P.I. specimens with MAPC were placed in the natural environment (20°C, 95% relative humidity) for 360 d. The 21 specimens were then immersed in a solution containing 10% Na_2SO_4 for 360 d.

2.3.1 *Flexural strength* The flexural strength of the repaired specimens with MAPC was measured using a universal testing device model (TYE-300F, China). The testing rate was 5 mm/min. Flexural strength of specimens was determined at ages of 7 d, 28 d, 90 d, 240 d, and 360 d.

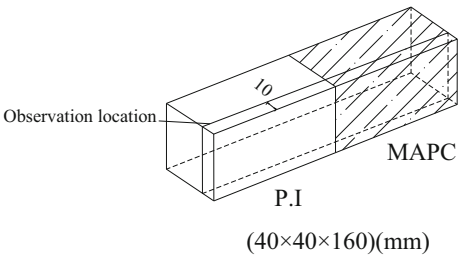

Figure 1. Bonded specimens.

2.3.2 *Morphology observation and microstructure test* The bonded specimens were cut to a surface distance of 10 mm (figure 1) in order to study changes of the interfacial transition zone under different conditions at different ages of 7 d, 28 d, 90 d, 240 d, and 360 d. Bonded specimen structures were observed using a 3D microscopic imaging system (LY-WN-YH, China). Bonded specimen microstructures were observed using SEM (JSM-5610LV, Japan). The bonded specimen with age of 360 d after flexural strength test was sampled at the cross section, and specimen phase composition was determined using X-ray diffraction (XRD, Bruker, Germany).

3. Results and discussion

3.1 *Flexural strength*

The repair quality of specimens repaired using MAPC can be determined by measuring flexural strength. If flexural strength of repaired specimens exceeds that of P.I specimens, the ability of MAPC to repair is concluded to be very good. The flexural strength results of the specimens in both environments are shown in table 3 and figure 2.

3.1.1 *Natural environment* Flexural strength was measured to determine the interfacial microzone strength

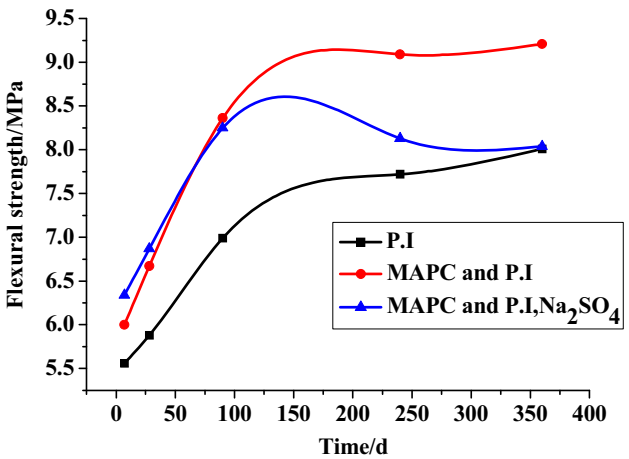

Figure 2. Flexural strength of specimens under different environments.

Table 3. Flexural strength of specimens under different environments.

	7 d	28 d	90 d	240 d	360 d
M0 (P.I)	5.36	5.88	6.99	7.72	8.01
M1 (MAPC and P.I)	6	6.67	8.36	9.09	9.21
M2 (MAPC and P.I, Na_2SO_4)	6.34	6.87	8.25	8.13	8.04

of MAPC on mortar. Flexural strength of MAPC repaired specimen is shown in figure 2. According to figure 2, flexural strength increased rapidly from 7 d to 28 d; while from 240 d to 360 d, flexural strength increased slowly. Therefore, increment of flexural strength was firstly significant and then not obvious. Specimens that had been repaired with MAPC had higher flexural strength compared with those repaired with Portland cement. The strength of the former specimens increased by 40% and 15% at 7 d and 360 d, respectively. Under the condition of the natural environment, hydration reactions continually occur within ordinary cement and bonded specimens, generating increasing amounts of hydration products. Thus, the internal structure of the specimens becomes more compact, increasing the flexural strength. Meanwhile, hydration speed and crystallization degree of MAPC are greater than that of Portland cement, and the needle hydration products of MAPC are more than that of ordinary cement, so the flexural strength of bonded specimens is higher than that of ordinary cement.

Therefore, MAPC was found to have a better repair effect than Portland cement. Although specimens repaired with both cements had increased flexural strength, those repaired with MAPC exhibited greater flexural strength. Therefore, the MAPC material has a greater bonding capacity.

3.1.2 *10% Na_2SO_4* The flexural strength of specimens repaired with MAPC and immersed in 10% Na_2SO_4 solution is shown in figure 2. The flexural strength increased at first, peaked at 90 d, and then decreased. The strength increased by 40% from 7 d to 90 d, and then decreased by 2% from 240 d to 360 d, and then continued to decrease slowly thereafter. Na_2SO_4 influenced the bond strength of the specimens repaired with MAPC, with the bond strength increasing at first and then decreasing. Although the link between Portland cement and MAPC was weak, the decrement was small.

This is primarily because the hydration reaction of MAPC immersed in 10% Na_2SO_4 solution is dominant. Therefore, the increased production of hydration products increases the flexural strength. With an extended corrosion time, the acid–alkali hydration reaction in MAPC mortar is gradually completed. The hydrolysis loss of hydration products formed in the samples of MAPC mortar soaked in 10% Na_2SO_4 solution begins to dominate, resulting in decreased MAPC mortar strength. However, the decrement is very small.

The hydration products of MAPC are relatively stable, closely combined with the Portland cement, and physical bonding is the main. There are few macroscopic defects in the interior and interface, which can guarantee the bond strength. Therefore, the binding capacity of MAPC is increasing at the initial stage. In the later stage of soaking, the excessive soluble phosphate in the MAPC gradually precipitated. At the same time, the two cement-based materials are corroded by sulphate for a long time, the strength gradually decreases, the structure becomes loose, and the bonding effect between the slurry and the matrix is weakened to a certain extent.

4. Microstructure

4.1 *Natural environment*

The microscopic appearance of the interfacial microzone after 28 d is shown in figure 3. In the interfacial microzone, the hydration products of the two cement materials penetrated into each other. There were many cracks on the repair surface of the Portland cement-based mortar specimens. Hydration products after repair of MAPC were found embedded in the micropores. The bond strength is determined primarily by cohesion and adhesion. The adhesion force is the interaction force between binder molecules. MAPC reacts with Portland cement hydrates and unhydrated clinker particles in Portland cement to produce gelatinous hydration products.

As shown in figure 4, the interfacial microzone of specimens exposed to the natural environment for 28 d is analysed according to backscatter electron diffraction scan. The partial large average atomic number indicates a strong backward scattering electron signal, resulting in bright shapes in the diagram. Part of the small average atomic number is a weak backward scattering electron signal, forming a dark zone in the diagram. The chemical composition of the sample is indicated by the contrast between brightness and darkness in the scan. The backscatter electron image shows the distribution of different components.

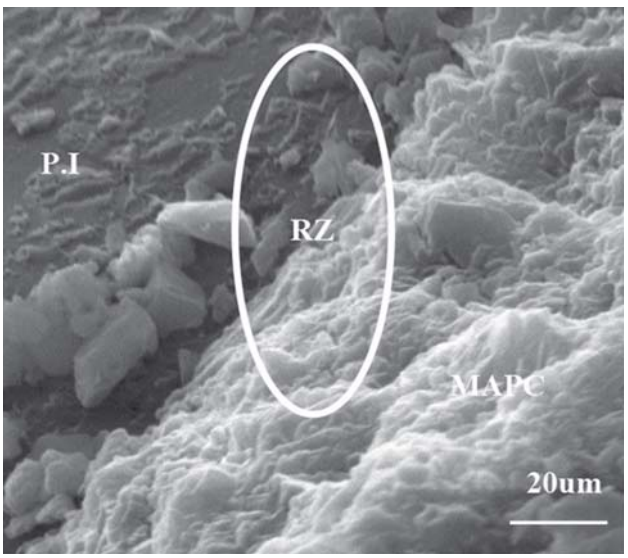

Figure 3. SEM of standard curing 28 d.

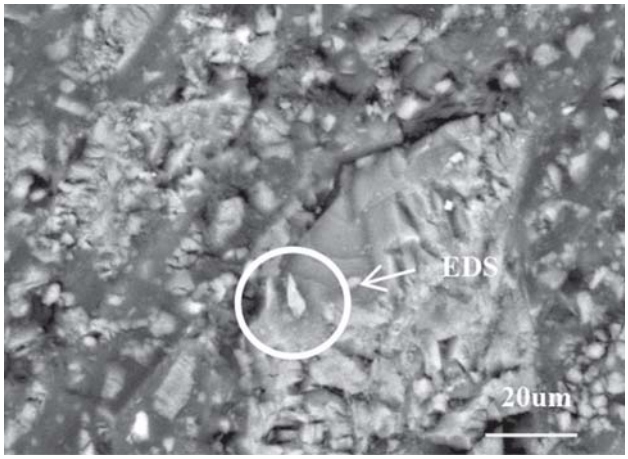

Figure 4. Diffraction pattern of the back scattered at the interface for 28 d.

Low-brightness zones indicate Portland cement matrix and bright zones are mainly composed of magnesium, phosphorus and other elements of MAPC repair materials. The two hydration products interweave and overlap closely at the interface to produce gel hydration products in the form of sheets or blocks, thus improving the bond strength.

An energy dispersive spectrometer (EDS) was used to analyse the elements of the bulk crystal, shown in figure 6; numerical results are provided in table 4. The EDS analysis indicates that the main elements of the bulk crystals include oxygen (O), phosphorus (P), nitrogen (N), magnesium (Mg) and calcium (Ca). The results show that different hydration products of the two types of cement-based materials can interact at the interface to form new amorphous products with gel properties, thus improving the interfacial bond strength.

4.2 *10% Na_2SO_4*

Figure 5 shows the microtopography of the interfacial microzone within specimens immersed in 10% Na_2SO_4 solution for 90 d and 360 d, respectively. After being soaked for 90 d in 10% Na_2SO_4 solution, the interface microzone hydration product appears relatively dense and contains no gaps. After 360 d, the structure of hydration product becomes fluffy and the pH value of the 10% Na_2SO_4 solution was 10. After 90 d, the stable MAPC hydration product merged with ordinary Portland cement through physical bonding. Few macro defects were found in the interface, indicating that bonding strength of the mortar is

Table 4. EDS of interface (wt%).

Ca	P	Mg	N	O
48.36	19.56	20.58	4.66	6.84

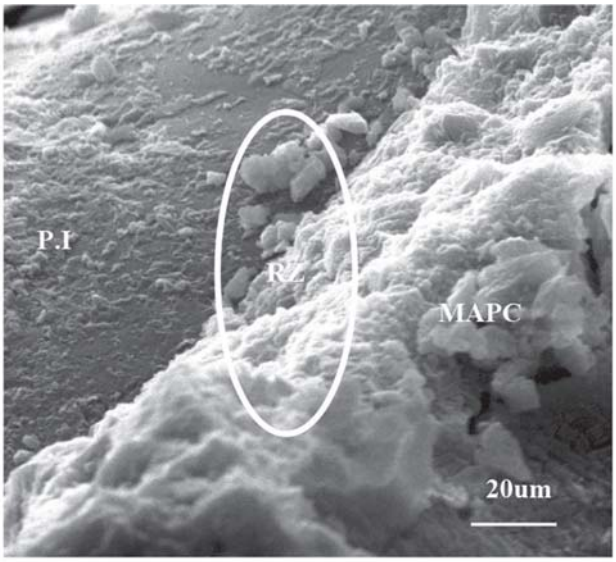

(a) 90 days

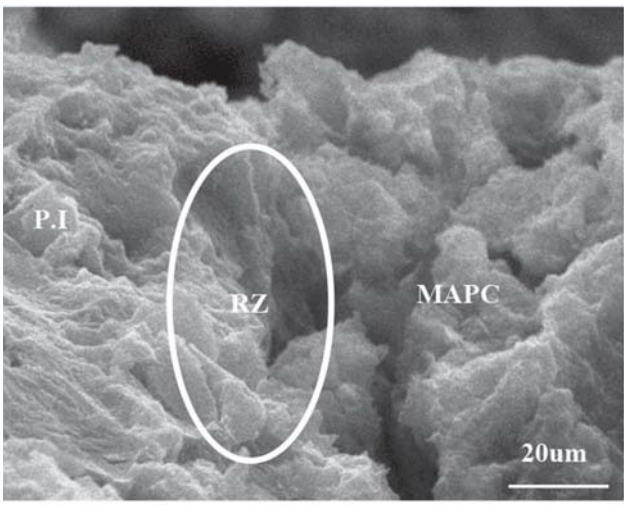

(b) 360 days

Figure 5. Micro topography at the interface of Na_2SO_4 solution.

good. The bonding ability of MAPC increased during the initial stage; thereafter, excess soluble phosphate from the MAPC gradually precipitated. Moreover, sulphate corrosion increasingly affected both types of cement over time, resulting in a gradual decrease in strength and a loose structure.

Figure 6 shows the XRD spectra for specimen interface microzone. The diffraction peaks of MgO and $MgNH_4PO_4{\cdot}6H_2O$ dominate the spectra, indicating that unhydrated $MgNH_4PO_4{\cdot}6H_2O$ and MgO appeared in the interface microzone during immersion in Na_2SO_4 solution. These compounds are vital to the MAPC bonding properties. In addition, a diffraction peak for a new product, $NaMg_3(OH)_2(CO_3)_2SO_4{\cdot}6H_2O$, appears in the spectra, which is an

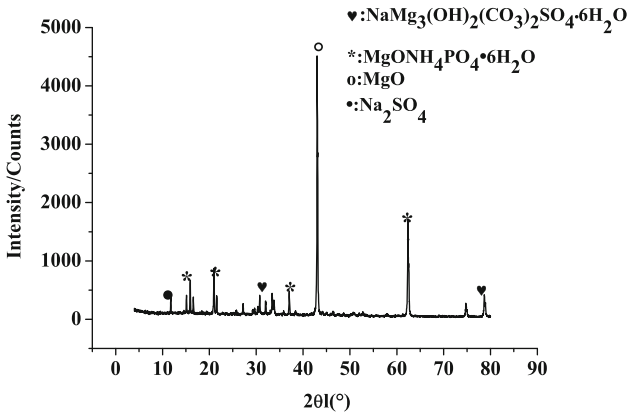

Figure 6. XRD of MAPC cross section in Na_2SO_4 for 360 days.

evidence of a reaction between the MAPC and the SO_4^{2-} anion in the Na_2SO_4 solution. The characteristics of the MAPC reflect complexities in the repair to the cement mortar interface microzone. In addition, the MAPC bonding capacity had decreased. The diffraction peak for Na_2SO_4 is due to the presence of Na_2SO_4 in the solution.

The bond strengths of the slurry and matrix also decreased. Fracture surface of the ruptured MAPC was scanned using XRD and SEM to analyse the interface microzone products.

Figure 7 illustrates the SEM spectra of the fractured surface of MAPC after exposure to the Na_2SO_4 solution. Flocculent glass dominates the hydration product and is mixed with needle-like crystals. Adjacent crystals comprise many cavities. The microstructure and group analysis indicate that the acicular crystal in the figure is Na_2SO_4, which mainly came from the solution. A small amount of Portland cement attached to the MAPC's fractured surface.

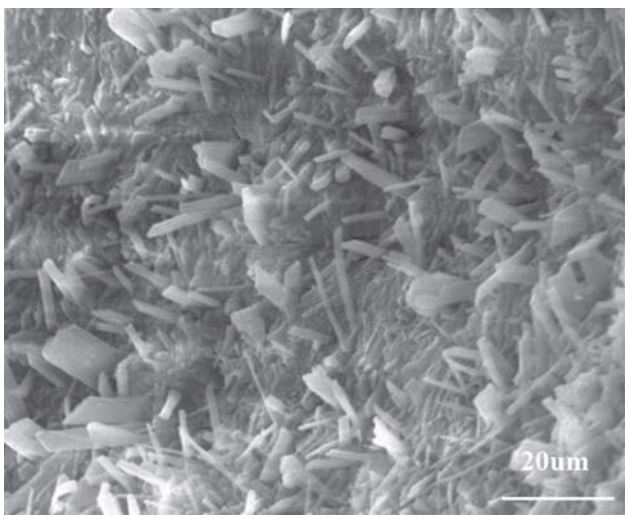

Figure 7. SEM of MAPC cross section in Na_2SO_4.

Therefore, the acicular crystals may also be calcium sulphoaluminate hydrate (referred to as ettringite, or AF). AF is generated from sulphate corrosion of Portland cement [19, 23] but could not be detected by XRD due to its negligible content. The flocculant colloid is the complex $NaMg_3(OH)_2(CO_3)_2SO_4{\cdot}6H_2O$. SEM analysis reveals great changes in the components and structure of the interface microzone of specimens immersed in Na_2SO_4 solution, as well as decreased MAPC bonding capacity.

4.3 *Chemical reactions*

Sodium sulphate reacts with Ca $(OH)_2$ in Portland cement paste to form calcium sulphate, which reacts with solid hydrated calcium aluminate in cement to form ettringite. The hydration product of MAPC, $MgNH_4PO_4{\cdot}6H_2O$, reacts with $Ca(OH)_2$ in Portland cement to form a new kind of cementitious product. After SEM analysis, the morphology of hydration products changed greatly.

In sodium sulphate solution, magnesium phosphate is mainly $MgNH_4PO_4{\cdot}6H_2O$. $MgNH_4PO_4{\cdot}6H_2O$ is the main hydration product of magnesium phosphate cement. It is a kind of gel. Through XRD analysis, there is also a diffraction peak of the new product, $NaMg_3(OH)_2(CO_3)_2SO_4{\cdot}6H_2O$. It shows that the magnesium phosphate coating reacts with SO_4^{2-} to form a new complex, $NaMg_3(OH)_2(CO_3)_2SO_4{\cdot}6H_2O$ in sulphate solution. This complex weakens the bond between the two cements.

5. Interfacial transition zone

The interfacial transition zone (ITZ) of MAPC is with low density and low strength due to the large pore and crystal size and marked crystal orientation in the transition zone. For this study, ITZ structure sketches of the MAPC in different environments have been drawn.

5.1 *Natural environment*

Within the mortar specimens exposed to the natural environment, the two cements hydrate at the interfacial microzone to produce substantial well-crystallized hydrates. The morphology and structure of the crystal in the ITZ remain unchanged with time. The interfacial zone structure is divided into three sub-zones:

(1) Contact layer and permeation layer: These layers include the interfacial chemical reaction products of the two cements, as well as pores and water film.
(2) Enrichment layer: This layer is characterised by a large number of pores and high porosity and is enriched with highly oriented $Ca(OH)_2$ crystals and struvite. Sketch of the ITZ structure is shown in figure 8.

5.2 Na_2SO_4

In the Na_2SO_4 solution, the hydrates in the ITZ are primarily flocculent and therefore the structure of the hydrates is loose. Although the crystal morphology changes with time, the MAPC exhibits a weakened bonding performance. Figure 9 shows the ITZ structure in Na_2SO_4.

There is a thick layer on the surface of the silicate structure where the MAPC and Portland cements contact. This is the precise contact layer. The struvite hydrate generated after 1 d of MAPC hydration is deposited on the matrix surface but is covered by a fine $Ca(OH)_2$ crystal layer. The struvite is perpendicular to the Portland cement surface. Later, a considerable amount of new hydrate continue to grow on the contact layer. The hydrate is also almost perpendicular to the surface of Portland cement and grows within the transition layer. The transition layer is composed mainly of the Portland and MAPC hydrates. As the hydration reaction progresses, the hydrates gradually solidify. Porosity of the transition layer reaches 50% in the final solidification state. Additionally, a group of tiny substances, mainly a collection of $Ca(OH)_2$ crystals whose faces are parallel to the aggregate surface, are distributed at the intermediate layer of this zone. The intermediate layer gradually moves to the aggregate surface until contact is achieved between the intermediate layer and the aggregate surface, thus showing an orientation and entering a dense cement paste structure. Acicular and rod-like hydrates are mainly distributed in the intermediate layer, and they cling and adhere substantially to the contact layer. The hydration products of the two cements and the new hydrates formed by inter reaction constitute most of the binding force.

Cracks appear in the contact layer with increasing age, leaving the aggregate surface exposed to crystallisation pressure. Hence, in the late age period (over 360 d), the binding force declines despite continuous increase in the strength of the cement paste.

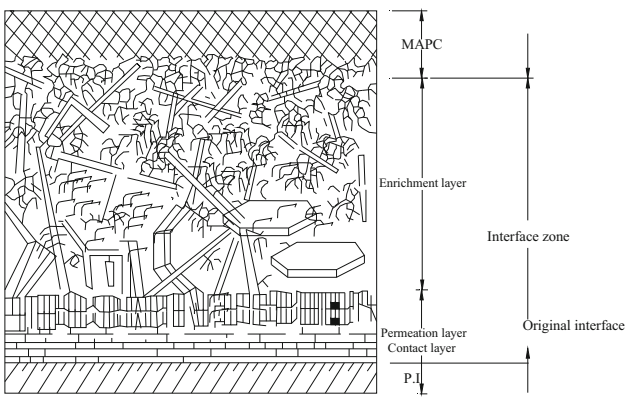

Figure 8. ITZ in natural environment.

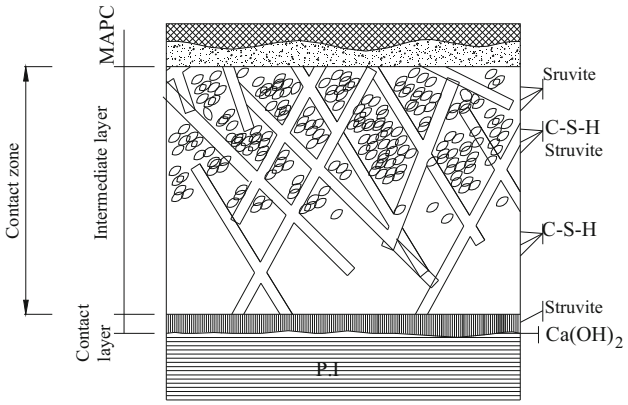

Figure 9. ITZ in Na_2SO_4.

6. Conclusions

(1) A distinct interfacial microzone exists between Portland cement and MAPC. Crystals with good crystallinity are formed in the interfacial microzone. The gel-like crystals are with excellent adhesion, indicating that the MAPC acts as a good repairing material.
(2) During the period of exposure to the natural environment, the two cements hydrate at the interfacial microzone to produce substantial well-crystallized hydrates. Neither the morphology nor the structure of crystals in the interfacial micro-zone undergoes significant changes over time.
(3) In the Na_2SO_4 solution, hydrates in the interface microzone are mostly flocculent, resulting in loose structure of the hydrates. Despite changes of the crystal morphology over time, the bonding performance of MAPC only declines slightly.
(4) The ITZ structure of the MAPC-bonded interface is divided into a contact zone, a permeation layer, an enrichment zone, and a weak effect zone. For both mortar specimens exposed to the natural environment and for those exposed to Na_2SO_4 corrosion, the microscopic characteristics of these zones changed significantly over time.

Acknowledgements

The authors would like to express their appreciations to Science and Technology Program of Henan Province of China (182102210418), and Key scientific research projects of universities in Henan (19B560004; 20B560010), and Kaifeng Science and Technology Program of Kaifeng City of China (1901023), and National Natural Science Foundation of China (51972337),and Funding for the high-level scientific research team of Kaifeng university, and Funded by the science and technology platform of Kaifeng

University collaborative innovation center for new energy-saving building materials.

References

[1] Jiang H and Chen C 2010 Influence of admixtures on the dissolution rate of chloride ion in magnesia cement. *Journal of Wuhan University of Technology* 32(18): 37–40

[2] Yang J M, Shi C J, Chang Y, et al. 2013 Hydration and hardening characteristics of magnesium potassium phosphate cement paste containing composite retarders. *Journal of Building Materials* 1: 43–49

[3] Li Y and Chen B 2013 Factors that affect the properties of magnesium ammonium phosphate cement. *Construction and Building Materials* 47: 977–983

[4] Soudee E and Pera J 2002 Influence of magnesia surface on the setting time of magnesia-phosphate cement. *Cement and Concrete Research* 32(1): 153–157

[5] Mestres G and Ginebra M 2011 Novel magnesium ammonium phosphate cements with high early strength and antibacterial properties. *Acta Biomaterialia* 7(4): 1853–1861

[6] Earnshaw R 1960 Investments for casting cobalt-chromium alloys, part I. *Br. Dent. J.* 108: 389–396

[7] Earnshaw R 1960 Investments for casting cobalt-chromium alloys, part II. *Br. Dent. J.* 108: 429–440

[8] Gaidis J M, Stierli R F and Tarver C C Magnesium phosphate concrete compositions. American patent: 3,960, 580,1976-6-1.

[9] Ding Z, Liu W and Xing F 2005 Property Study of High Early Strength Magnesium Phosphosilicate Cement. *The Seventh Council Meeting of the Chinese Ceramic Society*. 15(3): 1128–1135

[10] Quanbin Y, Shuqing Z, Qianrong Y, et al. 2000 Properties of new rapid repair material magnesium phosphate cement (in Chinese). *China Concrete and Cement Products*. 4(4): 8–11

[11] Yongchang H M et al 1989 *Corrosion and protection principles*. Shanghai: Shanghai Jiaotong University Press

[12] Dongxu L, Pengxiao L and Chunhua F 2009 Research on water resistance of magnesium phosphate cement (in Chinese). *Journal of Building Materials* 12(005): 505–510

[13] Yang Q, Zhang S and Wu X 2002 Deicer-scaling resistance of phosphate cement-based binder for rapid repair of concrete. *Cement and Concrete Research* 32(1): 165–168

[14] Jiang J, Xue M and Wang H 2012 Research on preparation and properties of marine magnesium phosphate cement based materials. *Journal of Functional Materials* 43(7): 828–830

[15] Laire Z, Qian J and Lu Z 2012 Effects of different temperature treatment to properties of magnesium phosphate cement. *Journal of Functional Materials* 43(15): 2035–2070

[16] Li D, Li P and Feng C 2009 Research on water resistance of magnesium phosphate cement. *Journal of Building Materials* 12(5): 505–510

[17] Yang Q, Zhu B and Wu X 2000 Characteristics and durability test of magnesium phosphate cement-based material for rapid repair of concrete. *Materials and Structures* 33(4): 229–234

[18] Brantschen F, Faria D M V and Ruiz M F 2016 Bond behaviour of straight, hooked, U-shaped and headed bars in cracked concrete. *Structural Concrete* 17(5): 799–810

[19] Zhu C, Chang X, Men Y and Luo X 2015 Modeling of grout crack of rockbolt grouted system. *International Journal of Mining Science and Technology* 25: 73–77

[20] Alireza G and Fall M 2016 Strength evolution and deformation behaviour of cemented paste backfill at early ages: Effect of curing stress, filling strategy and drainage. *International Journal of Mining Science and Technology* 26(5): 809–817

[21] Prince M J R and Singh B 2015 Bond behaviour of normal- and high-strength recycled aggregate concrete. *Structural Concrete* 16(1): 56–70

[22] Li J, Ji Y-s and Huang G 2017 Retardation and reaction mechanisms of magnesium phosphate cement mixed with glacial acetic acid. *RSC Advances* 7(74): 46852–46857

[23] De Villiers J P, van Zijl G P A G and van Rooyen A S 2017 Bond of deformed steel reinforcement in lightweight foamed concrete. *Structural Concrete* 18(3): 496–506